Single-Shot, Motion Insensitive Cardiac Imaging on a Standard Clinical System

M. Elizabeth Meyerand, Chad H. Moritz, Eric C. Wong

The overall goal of this study was the development and application of a less motion sensitive, single-shot MRI technique for use on a standard clinical system in a dynamic imaging setting, such as cardiac scanning. Time encoding, a single-shot line scanning technique, has been used to produce single-shot, small field-of-view cardiac images without the use of presaturation pulses. The major advantages of this method are: (1) as a line scanning technique, time encoding is minimally sensitive to motion when compared with 2D Fourier methods, and (2) aliasing will not occur if the object being imaged extends beyond the field of view.

Key words: single-shot MRI; line scanning; time encoding; cardiac imaging.

INTRODUCTION

Many MRI methods have been developed to investigate cardiac wall motion through the use of tagging techniques (1–3). Fast gradient echo methods have been created to create movies of heart motion (4–11). With additional hardware, echo-planar imaging (EPI) has been used in many research studies for single-shot cardiac imaging (12–15).

Cardiac triggered or ECG gated MRI has several practical problems (16). Because an ECG signal is required for gating, extra time must be alloted to position the ECG electrodes on the patient. The ECG signal can change once the patient is placed in the magnetic field, and the electrodes may then have to be repositioned. In addition, the patient's heart rate will most likely not remain constant throughout the scan, so some extra time must be allotted before each R wave to compensate for this effect. This requires that the duration of the data acquisition can be no longer than the minimum R-R interval. As a result, images cannot be obtained immediately before the R wave (late diastole), which is exactly the time period that is of most interest in cardiac examinations for the determination of ejection fraction, stroke volume, and diastolic filling rate (16). These complications can be avoided if the data are acquired in a single shot.

Time encoding is a single-shot technique involving non-Fourier encoding in one dimension and traditional Fourier encoding in the second dimension. Because specific details of the pulse sequence and image characteristics have been described previously (17–19), we will not discuss them here. The method is termed time encoding because the occurrence of an echo in time is directly related to the physical position of its corresponding line in space. One dimension is encoded in time and corresponds to a unique line in space. Therefore, aliasing will not occur in that dimension, even if the object being imaged extends beyond the FOV. If one is interested in obtaining images of a small portion of an anatomical region, time encoding can be used instead of conventional antialiasing techniques, such as using presaturation pulses. The additional time required for spatial saturation pulses may be very undesirable when the goal of the experiment is to rapidly acquire a series of images for a dynamic study. Heterogeneity of tissue characteristics and variations in B_1 can lead to incomplete nulling of outside signal when combinations of flip angles and saturation times are used. Hence, partial voluming of undesired tissue will always be a factor when spatial saturation is used and time encoding provides an alternative that avoids this problem.

Since time encoding is fundamentally a single-shot line scanning technique (20–30) any motion artifacts produced in an experiment will be spatially restricted to the line (time) when they occurred. This is contrasted to techniques utilizing 2D Fourier encoding where each point in k-space contains information about the entire image. With 2D Fourier encoding, any effects due to motion are distributed throughout the final image as blurring or ghosting.

Time encoding also resembles the class of Burst pulse sequences. With Burst sequences, a train of low flip angle RF pulses is used to excite multiple coherences creating an image in a single shot. However, unlike time encoding, the Burst techniques require a 2D Fourier transform for image reconstruction (31–34).

We have shown that the time encoding technique yields a reduction in motion related artifacts relative to other 2D Fourier transform single-shot techniques (17–19). Here we demonstrate the use of time encoding to produce single-shot, small FOV cardiac images without the use of additional hardware. Cardiac structures, such as the ventricular and atrial walls and septum, are visualized throughout the cardiac cycle.

METHODS

In vivo cardiac experiments were performed on five healthy volunteers (median age of 25). The time encoding sequence shown in Fig. 1 was used for these experiments at both 0.5 T and 1.5 T using GE Signa scanners.

MRM 40:930–933 (1998)

Biophysics Research Institute (M.E.M.), Medical College of Wisconsin, Milwaukee, Wisconsin; Department of Radiology and Psychiatry (C.H.M., E.C.W.), University of California at San Diego, San Diego, California.

Address correspondence to: M. Elizabeth Meyerand, Ph.D., Biomedical NMR Research Lab, Dartmouth-Hitchcock Medical Center, 7786 Vail Building, Room 712, Hanover, NH 03755.

Received July 28, 1997; revised April 1, 1998; accepted April 29, 1998.

0740-3194/98 $3.00

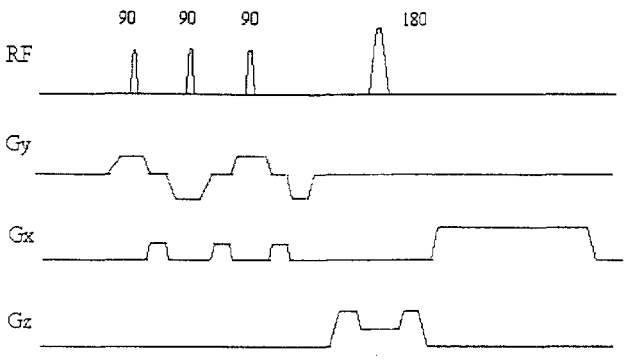

FIG. 1. The time encoding pulse sequence. Note that the 90° RF pulses are offset in frequency to select a different contiguous plane in *y*. The number of 90° pulses will equal the desired matrix size in the time encoding direction (which, as shown in this figure, would equal 3).

The sequence begins with the selection of contiguous parallel planes along the time encoding direction. These planes will form lines in the resultant time encoding image after the 180° slice selection pulse. Therefore, the number of slice selective RF pulses will equal the desired matrix size in the time encoding direction. After each plane selection gradient lobe, a blip gradient is applied in an orthogonal direction. The purpose of this gradient is to impart an incremental 2ΠN phase twist across a line so that adjacent lines can be differentiated from each other. The blips have an additive effect. Thus, the first plane selected in the pulse sequence will have a phase twist along its length created by all of the blips in the pulse sequence. Although this first plane has the highest amount of phase twist, the last plane to be selected has the least amount of phase twist because it is affected only by the final blip in the sequence. The slice selective 180° pulse then creates a slice through the contiguous parallel planes after the time encoding portion of the sequence has been completed. The linear read gradient tilts the phase plane so that each line that has a different amount of phase twist will read out at a different time. The end result is a train of spin echoes, each having a different TE and each arising from adjacent physical strips of tissue. The nominal TE of the sequence was chosen as the time between the 180° pulse and the middle of the echo train.

The standard GE body gradient coil and body RF coil were used in all experiments. As a single-shot method, retrospective gating was used. A series of gradient echo images were acquired first to select a plane for the time encoding study.

For the time encoding experiments, a nominal TE of 40 ms was chosen along with a TR of 1.5 s. The relatively long TR was chosen to prevent saturation, since the technique uses spin echoes. The acquisition window was 15 ms, resulting in a collection time of 234 μs for each of the samples collected in a single shot. The matrix size was 64 × 16, FOV = 48 cm × 12 cm, an RF pulse duration of 100 μs, and an image slice thickness = 5 mm. The final images were interpolated to 256 × 64.

RESULTS

Figure 2 shows a series of axial images acquired in progressively more inferior locations down the axis of the heart, beginning at the level of the aortic arch. In all five volunteers, the four chambers were clearly visible. In

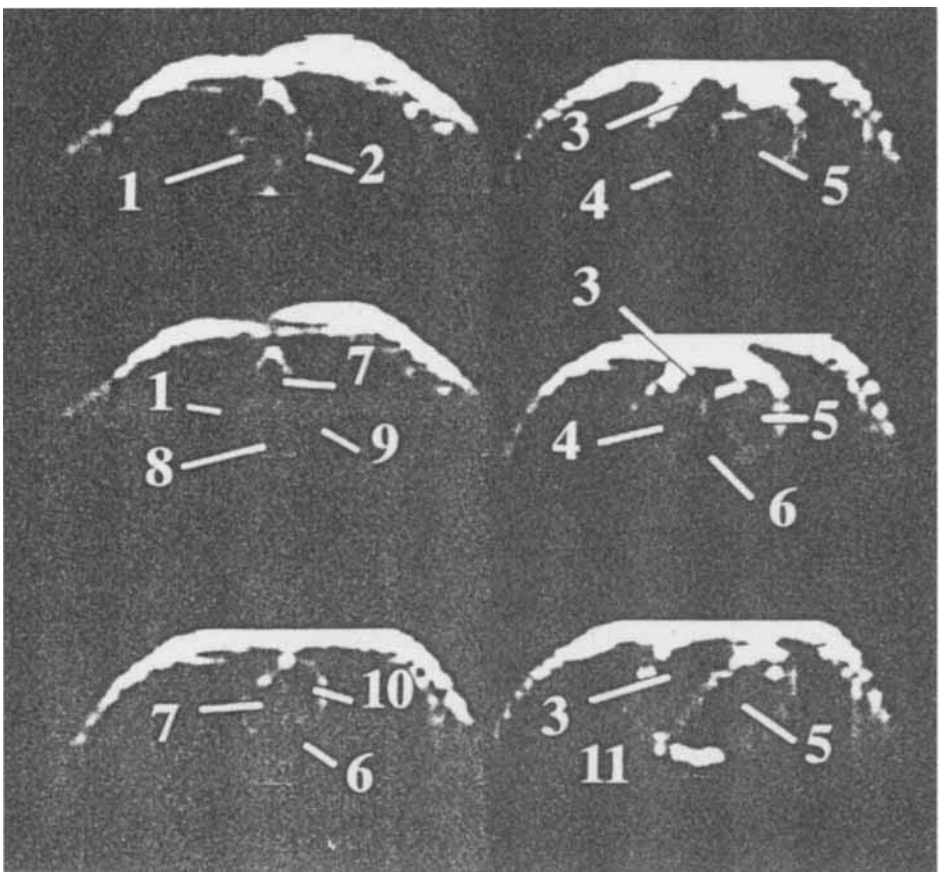

FIG. 2. A series of axial images progressing from superior to inferior locations along the long axis of the heart beginning at the level of the aortic arch. The images have been displayed in columns starting in the upper left and ending in the lower right. The imaging parameters were: nominal TE = 40 ms, FOV = 48 cm × 12 cm, matrix = 64 × 16 (interpolated to 256 × 64), slice thickness = 5 mm. Anatomical locations are numbered as follows: 1 = superior vena cava, 2 = aortic arch, 3 = right ventricle, 4 = right atrium, 5 = left ventricle, 6 = left atrium, 7 = ascending aorta, 8 = trachea, 9 = descending aorta, 10 = right ventricular outflow region, and 11 = diaphragm.

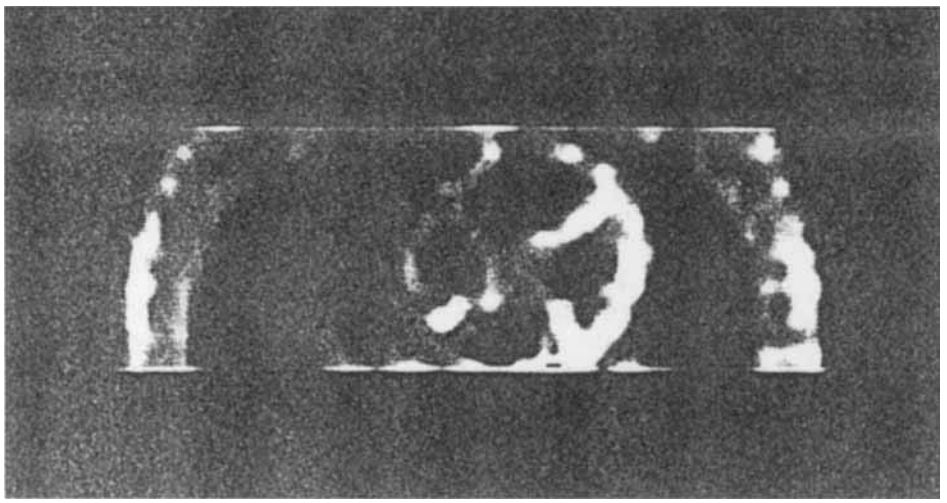

FIG. 3. Four-chamber view of the heart during systole, which has been multiplied by an exponential mask to correct for the spatially varying T_2 effect in the time encoding (y) direction. Notice that the signal intensity is more uniform in y in this corrected image. Imaging parameters were: nominal TE = 40 ms, FOV = 48 cm × 12 cm, matrix = 64 × 16 (interpolated to 256 × 64), slice thickness = 5 mm.

general it seems that diastolic images facilitated delineation of ventricular structures, whereas the valves were better visualized in their closed position during systole.

Assuming a relatively uniform T_2 across the FOV, a mask can be created for the cardiac images to correct for the y dependent decrease in signal intensity due to T_2. Figure 3 shows the image with the four-chamber view after the application of an exponential mask of the form $\exp(t/T_2)$ where T_2 of the heart is 55 ms.

The b value also varies in a time encoding image along the time encoding direction where $b_i \sim \gamma^2 G^2 TE_i^3/12$ and where TE_i is the TE of each echo (17). However, the attenuation due to diffusion alone is quite small because clinical gradient strengths of only 1 G/cm are being used along with relatively short TE values. In fact, the variation in b values from one side of the image to the other (in y) amounts to only a 0.1% change in signal, assuming a published value for the apparent diffusion coefficient in the heart along y of 1.48 mm^2/s (35).

DISCUSSION

Single-shot cardiac images were acquired using time encoding with standard clinical hardware. Cardiac gating and averaging were not used. Cardiac structures were visible in the time encoded images. The signal-to-noise ratio (SNR) in separate phases of the heart cycle averaged 25, allowing acceptable viewing of cardiac structures.

A mask approximating the T_2 decay of heart at 1.5 T was applied to the time encoded images to correct for T_2-related signal attenuation. Time encoding techniques can also be used to measure apparent diffusion coefficients.

Although less sensitive to motion effects, as a line scan technique time encoding suffers from a decrease in the SNR equal to the square root of the number of lines compared with a 2D-technique. Yet, as a line scan technique, the FOV can be greatly decreased in the time encoding direction, as well as in the frequency encoding direction, allowing imaging of objects that extend beyond the FOV in both directions.

The ultimate resolution of the technique is dependent on the slice profile of each excitation pulse. Therefore, an improvement in the RF slice profile will improve the resolution but with an added time penalty. The T_2 decay of the signal primarily affects the number of time encoded lines that can be collected in each experiment and thus has an indirect effect on the number of lines in the time encoding direction. This restriction is unlike that for gradient echo EPI where T_2^* decay degrades the spatial resolution. Like EPI, faster gradient ramp times and higher gradient strengths make higher resolutions achievable. In addition, if the resolution of the time encoding sequence is increased so that the time beween the slice selective RF pulses becomes longer than the time scale of the motion of the tissue, we will see the line-to-line motion artifact present with line scanning methods.

As a line scan technique, time encoding has been used successfully to image anatomy that extends beyond the field of view without the aliasing that accompanies 2D Fourier methods. Using small fields of view, time encoding can be used to obtain high resolution, single-shot images of individual sections within the heart.

REFERENCES

1. E. R. McVeigh, E. A. Zerhouni, Noninvasive measurement of transmural gradients in myocardial strain with MR imaging. *Radiology* **180,** 677–683 (1991).
2. E. R. McVeigh, E. Atalar, Cardiac tagging with breath-hold cine MRI. *Magn. Reson. Med.* **28,** 318–327 (1992).
3. C. C. Moore, W. G. O'Dell, E. R. McVeigh, E. A. Zerhouni, Calculation of three-dimensional left ventricular strains from biplanar tagged MR images. *J. Magn. Reson. Imaging* **2,** 165–175 (1992).
4. D. J. Atkinson, R. R. Edelman, Cineangiography of the heart in a single breath hold with a segmented turboFLASH sequence. *Radiology,* **178,** 357–360 (1991).
5. B. Chapman, R. Turner, R. J. Ordidge, M. Doyle, M. Cawley, R. Coxon, P. Glover, P. Mansfield, Real-time movie imaging from a single cardiac cycle by NMR. *Magn. Reson. Med.* **5,** 246–254 (1987).
6. M. S. Cohen, R. M. Weisskoff, R. R. Rzedzian, Clinical methods for single-shot instant MR imaging of the heart. *Radiology* **173(P),** 359 (1989).
7. E. Drucker, I. L. Pykett, R. R. Rzedzian, S. Miller, R. E. Dinsmore, Preliminary evaluation of a new high-speed MR imaging system for the assessment of cardiac function in normal volunteers, *in* "Proc., SMRM, 6th Annual Meeting, New York 1987," p. 17.
8. J. Frahm, A. Haase, K. D. Matthaei, Rapid three-dimensional imaging using the FLASH technique. *J. Comput. Assist. Tomogr.* **10,** 363–368 (1986).
9. J. Frahm, A. Haase, K. D. Matthaei, Rapid NMR imaging of dynamic processes using the FLASH technique. *Magn. Reson. Med.* **4,** 162–174 (1987).
10. J. Frahm, K. D. Merboldt, H. Bruhn, M. L. Gyngell, W. Hanicke, D.

Chien, 0.3-Second FLASH MRI of the human heart. *Magn. Reson. Med.* **13,** 150–157 (1990).
11. A. Haase, J. Frahm, K. D. Matthaei, FLASH imaging: rapid NMR imaging using low flip angles. *J. Magn. Reson.* **67,** 258–266 (1986).
12. D. A. Leung, J. F. Debatin, S. Wildermuth, G. C. McKinnon, G. K. von Shulthess, Cardiac imaging: comparison of two-shot echo-planar imaging with fast segmented *k*-space and conventional gradient-echo cine acquisitions. *J. Magn. Reson. Imaging* **5,** 684–688 (1995).
13. R. M. Weisskoff, J. J. Dalcanton, R. R. Rzedzian, 40 msec instant long axis heart imaging, *in* "Proc., SMRM, 9th Annual Meeting, New York, 1990," p.123.
14. C. P. Davis, G. C. McKinnon, J. F. Debatin, D. Wetter, A. C. Eichenburger, S. Duewell, G. K. von Shulthess, Normal heart: evaluation with echo-planar MR imaging. *Radiology* **191,** 691–696 (1994).
15. I. L. Pykett, R. R. Rzedzian, Instant images of the body by magnetic resonance. *Magn. Reson. Med.* **5,** 563–571 (1987).
16. T. A. Spraggins, Wireless retrospective gating: application to cine cardiac imaging. *Magn. Reson. Imaging* **8,** 675–681 (1990).
17. M. E. Meyerand, E. C. Wong, A time encoding method for single-shot imaging. *Magn. Reson. Med.* **34,** 618–622 (1995).
18. M. E. Meyerand, E. C. Wong, A modified time encoding method for high resolution imaging, *in* "Proc., SMR, 3rd Annual Meeting, Nice, France, 1995," p.637.
19. M. E. Meyerand, C. H. Moritz, E. C. Wong, Single-shot, motion insensitive cardiac imaging on a standard clinical system, *in* "Proc., SMR, 3rd Annual Meeting, New York, 1996," p. 658.
20. D. C. Ailion, K. Ganesan, T. A. Case, R. A. Christman, Rapid line scan technique for artifact-free images of moving objects. *Magn. Reson. Imaging* **10,**747–754 (1992).
21. K. Butts, N. J. Hangiandreou, S. J. Riederer, Phase velocity mapping with a real time line scan technique. *Magn. Reson. Med.* **29,** 134–138 (1993).
22. D. G. Brown, S. J. Riederer, R. C. Wright, Y. Liu, F. Farzaneh, High-speed line scan MR angiography. *Magn. Reson. Med.* **15,** 475–482 (1990).
23. D. A. Feinberg, J. C. Hoenninger, L. E. Crooks, L. Kaufman, J. C. Watts, M. Arakawa, Inner volume MR imaging: technical concepts and their applications. *Radiology* **156,** 734–747 (1985).
24. D. A. Feinberg, P. D. Jakob, Tissue perfusion in humans studied by Fourier velocity distribution, line scan, and echo-planar imaging. *Magn. Reson. Med.* **16,** 280–293 (1990).
25. J. Frahm, K. D. Merboldt, W. Hanicke, M. L. Gyngell, H. Bruhn, Rapid line scan NMR angiography. *Magn. Reson. Med.* **7,** 79–87 (1988).
26. P. Mansfield, P. G. Morris, NMR Imaging in Biomedicine, pp. 101–107, Academic Press, New York, 1982.
27. D. Jensen, D. Holtz, SLIM—A novel approach to fast MR imaging, *in* "Proc., SMRM, 7th Annual Meeting, San Francisco, 1988," p. 117.
28. D. Jensen, D. Holtz, Contrast behavior and T1 estimation in the fast MR line scanning technique SLIM, *in* "Proc., SMRM, 8th Annual Meeting, Amsterdam, 1989," p. 835.
29. H. Gudbjartsson, SE Maier, RV Mulkern, IA Morocz, S Patz, FA Jolesz, Line scan diffusion imaging. *Magn. Reson. Med.* **36,** 509 (1996).
30. C. J. Hardy, J. D. Perlman, J. R. Moore, P. B. Roemer, H. E. Cline, Rapid NMR cardiography with a half-echo M-mode method. *Comput. Assist. Tomogr.* **15,** 868–874 (1991).
31. J. Hennig, Burst-imaging on a clinical whole body system, *in* "Proc., SMRM, 11th Annual Meeting, Berlin, 1992," p.101.
32. P. van Gelderen, C. T. W. Moonen, J. H. Duyn, Susceptibility insensitive single-shot MRI combining BURST and multiple spin echoes. *Magn. Reson. Med.* **33,** 439–442 (1995).
33. I. J. Lowe, R. E. Wysong, DANTE ultrafast imaging sequence (DUFIS). *J. Magn. Reson. B* **101,** 106–109 (1993).
34. L. Zha, R. E. Wysong, I. J. Lowe, Optimized ultra-fast imaging sequence (OUFIS), *in* "Proc., SMRM, 12th Annual Meeting, New York, 1993," p. 471.
35. R. R. Edelman, J. Gaa, V. J. Wedeen, E. Loh, J. M. Hare, P. Prasad, W. Li, *In vivo* measurement of water diffusion in the human heart. *Magn. Reson. Med.* **32,** 423–428 (1994).